

AD A 045095

12 B.S.

NBSIR 77-1304 (ARPA)

Optical Materials Characterization

Albert Feldman, Deane Horowitz and Roy M. Waxler

Inorganic Materials Division
Institute for Materials Research

and

Marilyn J. Dodge and Warren K. Gladden

Optical Physics Division
Institute for Basic Standards
National Bureau of Standards
Washington, D.C. 20234

DDC
OCT 11 1977
C

August 1977

Semi-Annual Technical Report
Period Covered: February 1, 1977 to July 31, 1977
ARPA Order No. 2620

AD No. _____
DDC FILE COPY

Prepared for
Advanced Research Projects Agency
Arlington, Virginia 22209

DISTRIBUTION STATEMENT A
Approved for public release;
Distribution Unlimited

NBSIR 77-1304 (ARPA)

OPTICAL MATERIALS CHARACTERIZATION

Albert Feldman, Deane Horowitz and Roy M. Waxler

Inorganic Materials Division
Institute for Materials Research

and

Marilyn J. Dodge and Warren K. Gladden

Optical Physics Division
Institute for Basic Standards
National Bureau of Standards
Washington, D.C. 20234



August 1977

Semi-Annual Technical Report
Period Covered: February 1, 1977 to July 31, 1977
ARPA Order No. 2620

Prepared for
Advanced Research Projects Agency
Arlington, Virginia 2209



U.S. DEPARTMENT OF COMMERCE, Juanita M. Kreps, *Secretary*

Dr. Sidney Harman, *Under Secretary*

Jordan J. Baruch, *Assistant Secretary for Science and Technology*

NATIONAL BUREAU OF STANDARDS, Ernest Ambler, *Acting Director*

OPTICAL MATERIALS CHARACTERIZATION

Albert Feldman, Deane Horowitz and Roy M. Waxler

**Inorganic Materials Division
Institute for Materials Research**

Marilyn J. Dodge and Warren K. Gladden

**Optical Physics Division
Institute for Basic Standards**

ARPA Order No. 2620
Program Code Number. 4D10
Effective Date of Contract January 1, 1974
Contract Expiration Date December 31, 1977
Principal Investigator Albert Feldman
(301) 921-2840

The views and conclusions contained in this document are those of the authors and should not be interpreted as necessarily representing the official policies, either expressed or implied, of the Advanced Research Projects Agency or the U.S. Government.

ACCESSION for	
NTIS	White Section <input checked="" type="checkbox"/>
DDC	Buff Section <input type="checkbox"/>
UNANNOUNCED	<input type="checkbox"/>
J S I ICA 104	
BY	
DISTRIBUTION/AVAILABILITY CODES	
SPECIAL	
A	

OPTICAL MATERIALS CHARACTERIZATION

Abstract

The refractive index of fusion cast CaF_2 was measured at room temperature over the wavelength range $0.2144 \mu\text{m}$ to $8.662 \mu\text{m}$ and the data were fitted to a Selmeier type equation. Measurements of refractive index of hot forged CaF_2 were extended to the wavelength range $0.2024 \mu\text{m}$ to $0.2483 \mu\text{m}$. Data are presented for dn/dT of single crystal specimens of CaF_2 , BaF_2 , reactive atmosphere processed (RAP) KCl and KBr , LiF , NaF , and SrF_2 , and polycrystalline chemical vapor deposited (CVD) ZnSe and ZnS . The measurements were done by the method of Fizeau interferometry over the temperature range -180° to 200°C at the wavelengths $0.6328 \mu\text{m}$, $1.15 \mu\text{m}$, $3.39 \mu\text{m}$ and $10.6 \mu\text{m}$. Data are presented for the refractive indices, the linear thermal expansion and dn/dT of Lexan and Plexiglas 55.

Table of Contents

1. Technical Report Summary	1
1.1 Technical Problem	1
1.2 General Methodology	1
1.3 Technical Results	2
1.4 Department of Defense Implications.	3
1.5 Implications for Further Research	3
2. Technical Report	4
2.1 Refractive Index of Fusion-Case Calcium Fluoride - Marilyn J. Dodge and Warren K. Gladden.	4
2.1.1 Introduction	4
2.1.2 Experimental Technique	4
2.1.3 Index Data	5
2.1.4 Conclusions.	7
2.1.5 References	8
2.2 Temperature Derivative of Refractive Index of Infrared Window Materials - Albert Feldman, Deane Horowitz and Roy M. Waxler	11
2.2.1 Introduction	11
2.2.2 Experimental Method.	11
2.2.3 Results and Discussion	12
2.2.4 References	12
3. Acknowledgments.	37

OPTICAL MATERIALS CHARACTERIZATION

1. Technical Report Summary

1.1 Technical Problem

Windows subjected to high-average-power laser radiation will undergo optical and mechanical distortion due to absorptive heating. If the distortion becomes sufficiently severe, the windows become unusable. Theoretical calculations of optical distortion in laser windows depend on the following material parameters; absorption coefficient, refractive index, change of index with temperature, thermal expansion coefficient, stress-optical constants, elastic compliances, specific heat, thermal conductivity and density. Our program has been established to measure refractive indices, changes of index with temperature, stress-optical constants, elastic compliances, and thermal expansion coefficients of candidate laser window materials.

1.2 General Methodology

Laboratory experiments are conducted for measuring refractive indices, changes of index with temperature, stress-optical constants, elastic compliances, and thermal expansion coefficients.

The refractive indices of prismatic specimens are measured on precision spectrometers by using the method of minimum deviation. Two spectrometers are used. One instrument, which uses glass optics, is used for measuring refractive indices in the visible with an accuracy of several parts in 10^6 . The other instrument, which uses mirror optics, is used for measuring refractive indices in the ultraviolet and the infrared to an accuracy of several parts in 10^5 . Using both spectrometers we can measure refractive indices over the spectral region $0.2 \mu\text{m}$ to $50 \mu\text{m}$.

We measure the coefficient of linear thermal expansion, α , by a method of Fizeau interferometry. The interferometer consists of a specially prepared specimen which separates two flat plates. Interference fringes are observed due to reflections from the plate surfaces in contact with the specimen. We obtain α by measuring the shift of these interference fringes as a function of temperature. We can measure α from -180°C to 800°C .

The change of refractive index with temperature, dn/dT , is measured by two methods. In the first method, we measure the refractive index with the precision spectrometers at two temperatures, 20°C and 30°C , by varying the temperature of the laboratory. This provides us with a measure of dn/dT at room temperature. The second method may be used for measuring dn/dT from -180°C to 800°C . We obtain dn/dT from a knowledge of the expansion coefficient and by measuring the shift of Fizeau

fringes in a heated specimen as a function of temperature. The Fizeau fringes are due to interferences between reflections from the front and back surfaces of the specimens.

We measure piezo-optic coefficients and elastic compliances using a combination of Twyman-Green and Fizeau interferometers. From the shift of fringes in specimens subjected to uniaxial or hydrostatic compression, we obtain the necessary data for determining all the stress-optical constants and elastic compliances.

In materials with small piezo-optic constants or in materials that cannot withstand large stresses, we use interferometers designed to measure fractional fringe shifts. At 10.6 μm we use a modified Twyman-Green interferometer which has a sensitivity of 0.01λ . At 632.8 nm, we use a modified Dyson interferometer which has a sensitivity of 0.002λ . When using these interferometers to measure piezo-optic constants we must know the elastic constants of the material under test.

1.3 Technical Results

The refractive index of fusion cast CaF_2 was measured from 0.2144 μm to 8.662 μm at room temperature and the results were fitted to a Selmeier type equation. These results agreed well with earlier measurements on single crystal CaF_2 . In an extension of previously reported measurements, the refractive index of hot forged CaF_2 was measured from 0.2024 μm to 0.2483 μm .

We present data of dn/dT that we have obtained for the following materials at the specified wavelengths:

	.6328 μm	1.15 μm	3.39 μm	10.6 μm
BaF_2	x	x	x	x
CaF_2	x	x	x	
KBr (RAP)*	x	x	x	x
KCl (RAP)*	x	x	x	x
LiF	x	x	x	
NaF	x	x	x	
SrF_2	x	x	x	x
ZnS (CVD) ⁺		x	x	x
ZnSe (CVD) ⁺	x	x	x	x

* reactive atmosphere processed

⁺ chemical vapor deposited.

The measurements were made by the method of Fizeau interferometry over the temperature range -180° to 200° C. All the measurements on ZnS (CVD) and the measurements at $1.15 \mu\text{m}$ and $10.6 \mu\text{m}$ on the other materials are new. The other numbers were included in our previous report but are included here for completeness.

In addition to the above measurements on potential laser window materials, we have measured the refractive index, the linear thermal expansion coefficient and dn/dT of Plexiglas 55 and Lexan, materials used in the construction of aircraft windows. This work was done at the request of Captain Hurst of the Air Force Materials Laboratory at Wright-Patterson Air Force Base. The thermal expansion coefficient and dn/dT of Plexiglas 55 had been presented in our previous report, but the values for dn/dT were found to have a small error so we present the corrected values in this report.

1.4 Department of Defense Implications

The Department of Defense is currently constructing high-power laser systems. Criteria are needed for determining the suitability of different materials for use as windows in these systems. The measurements we are performing provide data that laser system designers can use for determining the optical performance of candidate window materials.

1.5 Implications for Further Research

We plan to complete the interferometric measurements of dn/dT and photoelastic constants in the infrared. We plan to measure dn/dT of NaCl and MgF_2 at $.6328 \mu\text{m}$, $1.15 \mu\text{m}$, $3.39 \mu\text{m}$, and $10.6 \mu\text{m}$. We plan to measure the photoelastic constants of CaF_2 , BaF_2 , and SrF_2 at $3.39 \mu\text{m}$.

Measurements of refractive index will be completed on ZnS (CVD) through the infrared. Refractive index measurements on MgF_2 will be started.

Apparatus will be assembled for measuring photoelastic constants and dn/dT in the ultraviolet. We are awaiting the arrival of an argon ion laser for measurements at 351 nm . We have procured a frequency doubler for producing 257 nm radiation from the argon ion laser line at 514 nm . After the system is assembled we plan to start measuring dn/dT and photoelastic constants on fused SiO_2 , Al_2O_3 , and CaF_2 .

2. Technical Report

2.1 Refractive Index of Fusion-Cast Calcium Fluoride

Marilyn J. Dodge and Warren K. Gladden

2.1.1 Introduction

The search for improved transparent optical component materials to be used in large, high-resolution systems incorporating high-power lasers has resulted in the development of new techniques for material fabrication. Hot-forging and fusion-casting [1]¹ are two techniques developed for the fabrication of alkaline-earth fluorides including calcium fluoride. Refractive index measurements from 0.25 μm to 8.0 μm have been previously reported [2] for a sample of Harshaw² hot-forged CaF_2 . Since that report, the wavelength range of index determinations on this sample have been extended to 0.2 μm .

A large prismatic sample of Raytheon developed fusion-cast CaF_2 was provided by Raytheon Corporation for refractive index measurement. The prism has a refracting angle of approximately 70° and two polished faces about 2.5 cm x 4 cm. Measurements have been made on this specimen from 0.2144 μm to 8.662 μm .

2.1.2 Experimental Technique

A precision spectrometer, shown schematically in figure 1 [3], was used to determine refractive index by means of the minimum-deviation method. From the ultraviolet to 2.0 μm , the index was determined at known emission wavelengths of mercury, cadmium, helium, and zinc. Beyond 2 μm , a glo-bar was used for the radiant-energy source and measurements were made at known absorption bands of water, carbon dioxide, polystyrene and 1,2-4 trichlorobenzene. A series of narrow-band interference filters was also used between 3.5 μm and 6.5 μm . A thermocouple with a cesium iodide window was used for signal detection in the visible and infrared and a photo-multiplier tube was used for the detector in the ultraviolet. The scale of this spectrometer can be read to 1.0 second of arc. The accuracy of this scale permits the determination of the refractive index of good optical quality material to within 2×10^{-5} over a wide wavelength range.

1. Figures in brackets indicate the literature references at the end of this paper.

2. The use of company and brand names in this paper are for identification purposes only and in no case does it imply recommendation or endorsement by the National Bureau of Standards and it does not imply that the materials used in this study are necessarily the best available.

The index of the cast CaF₂ was determined from 0.214438 to 8.662 μm at an average controlled room temperature near 21.7°C. Additional index data were obtained for the hot-forged CaF₂ from 0.202458 μm to .25 μm at 21.0°C.

The experimental data for the fusion-cast specimen was fitted to a three-term Sellmeier-type dispersion equation [4] of the form $n^2 - 1 = \sum [A_j \lambda^2 / (\lambda^2 - \lambda_j^2)]$, and a new fit was obtained for the hot-forged CaF₂. The index of refraction is represented by n , λ is the wavelength of interest in μm, the λ_j 's are the calculated wavelengths of maximum absorption and the A_j 's are the calculated oscillator strengths corresponding to the absorption bands. The λ_j 's and A_j 's are not intended to have any physical significance. Primary emphasis is given to procuring a mathematical fit of the measured data useful for interpolation.

2.1.3 Index Data

The constants calculated for each dispersion equation, the number of wavelengths fitted and the average absolute residual (the average difference between the experimental values and the calculated values) are given in table 1.

Table 1: Constants for Dispersion Equations for CaF₂

<u>Constant</u>	<u>Hot-Forged 20.8°C</u>	<u>Fusion-Cast 21.7°C</u>
A ₁	0.36648840	0.3439319
A ₂	0.6724568	0.6948269
A ₃	4.9928893	3.8902192
λ ₁	0.0167162	0.0127821
λ ₂	0.0946259	0.0936663
λ ₃	39.2563990	34.82590
No. of wavelengths	75	60
Wavelength range of fit	0.2267-8.03 μm	0.2144-8.662 μm
Average absolute residual of index x 10 ⁵	2.8	2.1

The average absolute residual is an indication of the overall accuracy of the experimental data. Generally, the largest residuals were in the IR beyond 5 μm, where 35 strong atmospheric absorption bands existed between 5.0 and 7.3 μm. Because of the large size of the prisms and the apparent excellent quality of both samples, these bands were sharp and

their minima were easily determined. Therefore, the index determinations are not considered to be any less accurate than in the UV or near IR. The wavelengths of these atmospheric bands were assigned from values in the literature[5,6]. The uncertainties in the wavelength values would be difficult to define due to differences in the laboratory conditions and the existence of many weak bands which could effect the wavelengths of nearby strong bands. An error of 0.1 % in wavelength would result in an index residual of 9×10^{-5} in this particular material.

The constants given in table 1 refer only to these two samples at the given temperature. Since the refractive index of samples of similar materials fabricated at different times can vary from one sample to another, caution should be used when either of these parameter sets is used to interpolate an index value at a specific wavelength for the purpose of describing another specimen. When using these parameters to obtain index values, interpolation should only be attempted within the wavelength range of the experimental data.

Although the hot-forged sample was measured at $0.202459 \mu\text{m}$, a mean of two Hg lines, a satisfactory fit could not be accomplished below $0.226747 \mu\text{m}$. When any of the 3 measured values at wavelengths below $.226746 \mu\text{m}$ were included in the fit, the λ_1 and λ_2 values increased to 0.077 and 0.192 respectively, which resulted in changes in the calculated index of the order of -1×10^{-4} at wavelengths up to $0.27 \mu\text{m}$ with large residuals in this region. This fitting-phenomena is characteristic when an attempt is made to fit experimental data close to a region of strong absorption to a Sellmeier-type equation. Although the absorption properties of this sample are not known in the spectral region around $.2 \mu\text{m}$, it appears that there could be an absorption in this area large enough to affect the refractive index to an extent that it can not be fitted. The final fit which was obtained resulted in λ_1 , λ_2 , A_1 and A_2 values which are close to those obtained for the fusion-cast sample, which would be expected. The λ_2 values are also close but below the known sharp ultraviolet cutoff of $.125 \mu\text{m}$ for single crystal CaF_2 [7].

The refractive index of each specimen was calculated at regular wavelength intervals by using the appropriate fitted parameters. The results for the fusion-cast material are plotted as a function of wavelength in figure 2.

The index values obtained for both types of material are compared in figure 3 with those obtained by I. H. Malitson on single crystal CaF_2 [8]. The single crystal data, corrected to 20.8°C is represented by the "zero" line. The difference in index between the single crystal and both the hot-forged CaF_2 and cast CaF_2 reaches a maximum close to $0.3 \mu\text{m}$. This index variance could be evidence of a weak absorption band near $0.3 \mu\text{m}$. The Harshaw catalog [7] shows transmission runs for two grades of CaF_2 , the UV grade in which this band does not appear, and the optical grade, sold for use in IR components, in which the band does exist. Assuming this band did not exist in the single crystal studied previously,

the difference in index would become more negative, reaching the maximum Δn , then receding as the index of the new CaF_2 approaches that of the single crystal in the red region of the spectrum. The refractive index of the fusion cast sample is within 1×10^{-5} of the index for the single crystal material between 1 and 8 μm , which is well within the experimental error of both sets of data. The refractive indexes of the cast material, measured at 21.7 $^\circ\text{C}$, were not corrected for temperature. However, since the accepted dn/dT ($^\circ\text{C}$) $^{-1}$ of CaF_2 is about -1×10^{-5} ($^\circ\text{C}$) $^{-1}$ [8], the effect on Δn of the cast sample caused by the temperature difference would be within the experimental error. The dip in the Δn curve for the forged sample was discussed in the earlier report [1]. Since this phenomenon is not exhibited by the cast material, it appears to be a property peculiar to the forged specimen.

2.1.4 Conclusions

The refractive index of hot-forged CaF_2 and fusion-cast CaF_2 are in good agreement from .3 μm to about 1.5 μm . The index of the fusion-cast material does not seem to be affected quite as much by the absorption in the UV as is the index of the forged specimen. Between 1 and 8 μm the fusion-cast sample has an index very close to the single crystal index, whereas the forged sample shows a change in index in the 5 μm region which might be related to an absorption effect. Without further study on other samples of hot-forged CaF_2 , it is not possible to determine if this phenomenon is peculiar to the particular sample in this study, or if it is the result of something in the fabrication technique.

2.1.5 References

1. Newberg, R. and Pappis, J., Fifth Annual Conference on Infrared Laser Window Materials, P. 1065, UDRI (Feb. 1976).
2. Dodge, M. J., "Laser Induced Damage in Optical Materials: 1976," P. 64, NBS Special Publication 462, U. S. Govt. Printing Office, Wash. (1976).
3. Rodney, William S. and Spindler, Robert J., J. Res. Nat'l. Bur. Stds. (US), 51, 123, (1953).
4. Sutton, Loyd E. and Stavroudis, Orestes N., J. Opt. Soc. Am. 51, 901 (1961).
5. Downie, A. R., Magoon, M. C., Purcell, Thomasine and Crawford, Bryce Jr., J. Opt. Soc. Am. 43, 941 (1953).
6. Benedict, W. S., Claassen, H. H. and Shaw, J. H., Res. NBS 49, 91 (1952).
7. Harshaw Optical Crystals, the Harshaw Chemical Co., 22, (1967).
8. Malitson, I. H., Applied Optics 2, 1103 (1963).

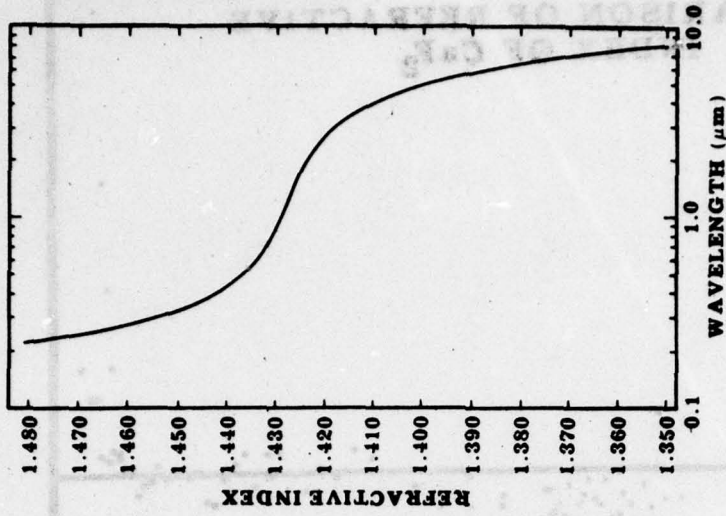


Fig. 2 Refractive index of fusion-cast CaF_2 as a function of wavelength (logarithmic scale). Data at 21.7°C were calculated from the dispersion equation of the form $n^2 - 1 = \sum A_j \lambda^2 / (\lambda^2 - \lambda_j^2)$.

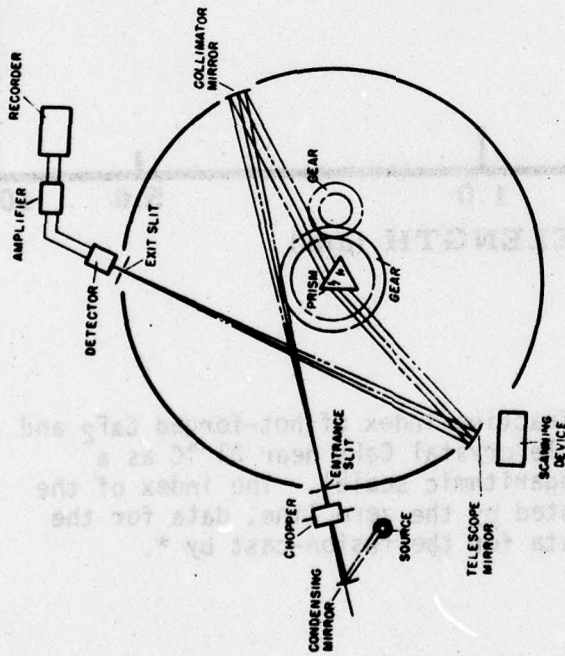


Fig. 1 Schematic diagram of the modified Gaertner precision spectrometer showing optical path. The prism is rotated at one-half the rotation rate of the telescope assembly by gear system, thus maintaining the condition of minimum-deviation for any wavelength. The scanning device drives the assembly which scans the spectrum to identify lines or bands and determine their approximate scale positions.

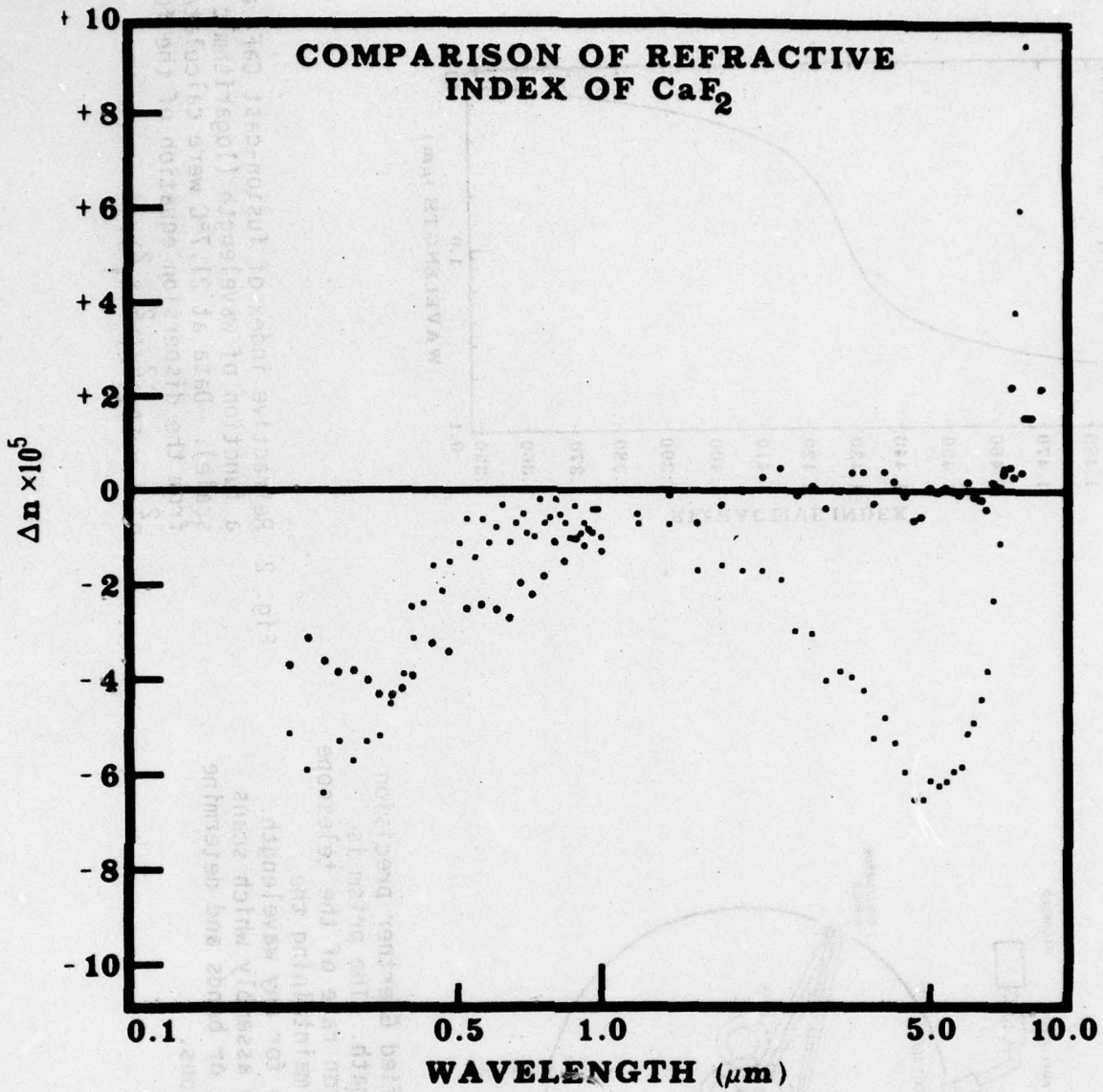


Fig. 3 The differences in the refractive index of hot-forged CaF₂ and fusion-cast CaF₂ from single crystal CaF₂ near 21 °C as a function of wavelength (logarithmic scale). The index of the single crystal is represented by the zero line, data for the hot-forged by the ■ and data for the fusion-cast by *.

2.2 Temperature Derivative of Refractive Index of Infrared Window Materials

Albert Feldman, Deane Horowitz and Roy M. Waxler

2.2.1 Introduction

When high-power radiation propagates through a laser window, the residual absorption causes a temperature rise in the window. The temperature distribution is, in general, nonuniform and hence, will distort the wavefront of the beam. The distortion arises from: the change of refractive index with temperature; the change of thickness with temperature; the change of refractive index and thickness caused by stresses produced by thermal gradients. In order to predict the distortion of a laser beam wavefront from the laser energy deposited in a window, one requires certain material parameters. These include the absorption coefficient, the refractive index n , the change of index with temperature dn/dT , the piezo-optic constants q_{ij} , the thermal expansion coefficient α , and the elastic constants s_{ij} or c_{ij} . It is the purpose of the Optical Materials Characterization Program at the National Bureau of Standards to measure n , dn/dT , q_{ij} and if necessary, α and s_{ij} .

In this report we present data of dn/dT on CaF_2 , BaF_2 , KBr (RAP), KCl (RAP), LiF, NaF, SrF_2 , ZnS (CVD), and ZnSe (CVD). The measurements were made over the temperature range $-180^\circ C$ to $200^\circ C$ at the wavelengths $0.6328 \mu m$, $1.15 \mu m$, $3.39 \mu m$ and $10.6 \mu m$, except that ZnS was not measured at $0.6328 \mu m$ due to excessive light scattering and CaF_2 , LiF, and NaF, were not measured at $10.6 \mu m$ because of absorption in the specimens. Some of the data were presented in our previous report, but are included here for completeness.

In addition, we present data on refractive index, the linear thermal expansion coefficient, and dn/dT of Plexiglas 55 and Lexan. The measurements were made at the request of Captain Hurst of the Air Force Materials Laboratory for determining the effect of heating caused by a nuclear explosion on the optical properties of aircraft windows. These measurements were supported in part by funds provided by the Air Force Materials Laboratory.

2.2.2 Experimental Method

We measured dn/dT and linear thermal expansion by the method of Fizeau interferometry, which has been described in detail in our previous report [1]. The refractive indices of Plexiglas 55 and Lexan were measured on a V-block refractometer [2].

2.2.3 Results and Discussion

In figures 4-12, we plot dn/dT as a function of temperature for CaF_2 , BaF_2 , KBr (RAP), KCl (RAP), LiF , NaF , SrF_2 , ZnS (CVD) and ZnSe (CVD). All of the specimens used were from single crystal material except for the ZnS and ZnSe which were polycrystalline. The points in each of the figures are the measured values. The data were fitted to a third degree polynomial in the temperature by the method of least squares and the results of the fit are tabulated in tables 2-10. The errors in the table are the standard deviation of the experimental data to the least squares fit. The refractive indices, the specimen thicknesses and references to the thermal expansion coefficient all of which were used in the computation of the results, are given in Table 11.

In figure 13 we show the linear thermal expansion coefficient of Lexan as a function of temperature. Figure 14 is a plot of dn/dT of Lexan as a function of temperature. In figure 15, we present a corrected plot of dn/dT as a function of temperature for Plexiglas 55. For completeness, we also give the linear thermal expansion coefficient of Plexiglas 55 as a function of temperature in figure 16. The refractive indices of Lexan and Plexiglas 55 at four wavelengths in the visible are presented in Table 12.

As discussed in our previous report, R. J. Harris, et al. [3] in a recent paper, presented dn/dT data on a series of materials including BaF_2 , CaF_2 , KCl , ZnS , and ZnSe . After correcting for their input parameters of refractive index and thermal expansion, we find good agreement between our values of dn/dT and their values for BaF_2 , CaF_2 , and KCl . However, there is disagreement in the values for ZnS and ZnSe . In a measurement on ZnSe at $0.6328 \mu\text{m}$ using an immersion technique similar to the technique used by Harris et al., we find that our newly measured values agree with our earlier measurement and disagree with the values of Harris et al.

2.2.4 References

- [1] A. Feldman, D. Horowitz, R. M. Waxler, M. J. Dodge, and W. K. Gladden, Optical Materials Characterization, National Bureau of Standards Internal Report, NBSIR 77-1219 (March 1977).
- [2] A. Feldman and D. Horowitz, J. Opt. Soc. Amer. **59**, 1406 (1969).
- [3] R. J. Harris, G. T. Johnston, G. A. Kepple, P. C. Krok, and H. Mukai, Appl. Optics **16**, 436 (1977).

Table 2. dn/dT of BaF_2 ($10^{-5}K^{-1}$)

Temperature (°C)	Wavelength (μm)			
	0.6328 ^a	1.15 ^b	3.39 ^b	10.6 ^b
-180	- .86	- .81	- .81	- .73
-160	- .98	- .96	- .95	- .85
-140	-1.09	-1.08	-1.07	- .96
-120	-1.19	-1.19	-1.17	-1.05
-100	-1.27	-1.29	-1.26	-1.13
- 80	-1.35	-1.37	-1.34	-1.21
- 60	-1.41	-1.44	-1.41	-1.27
- 40	-1.47	-1.50	-1.47	-1.32
- 20	-1.52	-1.55	-1.51	-1.37
0	-1.56	-1.59	-1.56	-1.41
20	-1.60	-1.62	-1.59	-1.45
40	-1.63	-1.66	-1.62	-1.48
60	-1.66	-1.69	-1.66	-1.51
80	-1.70	-1.71	-1.68	-1.54
100	-1.73	-1.74	-1.71	-1.57
120	-1.76	-1.77	-1.75	-1.60
140	-1.79	-1.80	-1.78	-1.63
160	-1.83	-1.84	-1.82	-1.66
180	-1.87	-1.88	-1.87	-1.70
200	-1.92	-1.93	-1.92	-1.75

^aStandard deviation from a third degree polynomial fit is 0.02

^bStandard deviation from a third degree polynomial fit is 0.03

Table 3. dn/dT of CaF_2 ($10^{-5}K^{-1}$)

Temperature (°C)	Wavelength (μm)		
	0.6328 ^a	1.15 ^a	3.39 ^b
-180	- .40	- .41	- .40
-160	- .54	- .56	- .52
-140	- .66	- .68	- .63
-120	- .77	- .78	- .73
-100	- .85	- .87	- .82
- 80	- .93	- .95	- .89
- 60	- .99	-1.01	- .95
- 40	-1.03	-1.06	-1.00
- 20	-1.07	-1.10	-1.05
0	-1.10	-1.13	-1.09
20	-1.13	-1.15	-1.12
40	-1.15	-1.18	-1.14
60	-1.17	-1.20	-1.17
80	-1.19	-1.22	-1.19
100	-1.21	-1.24	-1.21
120	-1.23	-1.26	-1.23
140	-1.26	-1.29	-1.25
160	-1.30	-1.32	-1.27
180	-1.34	-1.36	-1.30
200	-1.40	-1.41	-1.34

^aStandard deviation from a third degree polynomial fit is 0.02

^bStandard deviation from a third degree polynomial fit is 0.03

Table 4. dn/dT of KBr ($10^{-5}K^{-1}$)

Temperature (°C)	Wavelength (μm)			
	0.6328 ^a	1.15 ^a	3.39 ^a	10.6 ^b
-180	-2.95	-3.05	-3.05	-3.06
-160	-3.17	-3.26	-3.26	-3.24
-140	-3.36	-3.44	-3.44	-3.40
-120	-3.53	-3.59	-3.60	-3.54
-100	-3.67	-3.73	-3.74	-3.66
- 80	-3.78	-3.84	-3.85	-3.77
- 60	-3.88	-3.94	-3.95	-3.86
- 40	-3.96	-4.02	-4.03	-3.93
- 20	-4.02	-4.09	-4.10	-4.00
0	-4.08	-4.14	-4.16	-4.06
20	-4.12	-4.19	-4.21	-4.11
40	-4.16	-4.23	-4.25	-4.16
60	-4.19	-4.27	-4.29	-4.20
80	-4.23	-4.31	-4.33	-4.25
100	-4.27	-4.35	-4.36	-4.29
120	-4.31	-4.39	-4.40	-4.33
140	-4.36	-4.44	-4.44	-4.38
160	-4.42	-4.49	-4.49	-4.43
180	-4.49	-4.56	-4.55	-4.49
200	-4.58	-4.63	-4.62	-4.56

^aStandard deviation from a third degree polynomial fit is 0.03

^bStandard deviation from a third degree polynomial fit is 0.06

Table 5. dn/dT of KCl ($10^{-5}K^{-1}$)

Temperature (°C)	Wavelength (μm)			
	0.6328 ^a	1.15 ^a	3.39 ^a	10.6 ^b
-180	-2.32	-2.35	-2.39	-2.33
-160	-2.52	-2.55	-2.58	-2.50
-140	-2.70	-2.74	-2.75	-2.65
-120	-2.86	-2.90	-2.91	-2.80
-100	-3.00	-3.05	-3.05	-2.93
- 80	-3.13	-3.17	-3.17	-3.04
- 60	-3.24	-3.29	-3.28	-3.15
- 40	-3.35	-3.39	-3.38	-3.24
- 20	-3.43	-3.48	-3.47	-3.33
0	-3.51	-3.55	-3.55	-3.41
20	-3.58	-3.62	-3.62	-3.48
40	-3.65	-3.68	-3.69	-3.54
60	-3.70	-3.74	-3.75	-3.60
80	-3.76	-3.79	-3.80	-3.65
100	-3.81	-3.84	-3.85	-3.70
120	-3.86	-3.89	-3.90	-3.74
140	-3.91	-3.94	-3.94	-3.79
160	-3.96	-4.00	-3.99	-3.83
180	-4.02	-4.05	-4.04	-3.87
200	-4.08	-4.11	-4.09	-3.91

^aStandard deviation from a third degree polynomial fit is 0.02

^bStandard deviation from a third degree polynomial fit is 0.04

Table 6. dn/dT of LiF ($10^{-5}K^{-1}$)

Temperature (°C)	Wavelength (μm)		
	0.6328 ^a	1.15 ^b	3.39 ^b
-180	- .36	- .38	- .40
-160	- .63	- .64	- .60
-140	- .86	- .86	- .78
-120	-1.05	-1.05	- .93
-100	-1.21	-1.21	-1.06
- 80	-1.34	-1.34	-1.16
- 60	-1.44	-1.45	-1.25
- 40	-1.52	-1.53	-1.32
- 20	-1.59	-1.60	-1.37
0	-1.63	-1.65	-1.42
20	-1.67	-1.69	-1.45
40	-1.70	-1.73	-1.48
60	-1.72	-1.75	-1.51
80	-1.75	-1.77	-1.53
100	-1.78	-1.79	-1.56
120	-1.81	-1.81	-1.59
140	-1.85	-1.84	-1.63
160	-1.91	-1.88	-1.67
180	-1.99	-1.92	-1.73
200	-2.09	-1.99	-1.80

^aStandard deviation from a third degree polynomial fit is 0.02

^bStandard deviation from a third degree polynomial fit is 0.04

Table 7. dn/dT of NaF ($10^{-5}K^{-1}$)

Temperature (°C)	Wavelength (μm)		
	0.6328 ^a	1.15 ^a	3.39 ^a
-180	- .51	- .53	- .55
-160	- .67	- .71	- .69
-140	- .81	- .85	- .82
-120	- .92	- .96	- .92
-100	-1.00	-1.06	-1.00
- 80	-1.07	-1.13	-1.06
- 60	-1.12	-1.18	-1.11
- 40	-1.16	-1.21	-1.14
- 20	-1.19	-1.24	-1.17
0	-1.20	-1.25	-1.18
20	-1.21	-1.26	-1.19
40	-1.21	-1.26	-1.19
60	-1.22	-1.26	-1.19
80	-1.22	-1.26	-1.20
100	-1.22	-1.26	-1.20
120	-1.24	-1.27	-1.21
140	-1.26	-1.30	-1.23
160	-1.29	-1.33	-1.26
180	-1.33	-1.39	-1.30
200	-1.39	-1.46	-1.35

^aStandard deviation from a third degree polynomial fit is 0.05

Table 8. dn/dT of SrF_2 ($10^{-5}K^{-1}$)

Temperature (°C)	Wavelength (μm)			
	0.6328 ^a	1.15 ^b	3.39 ^c	10.6 ^d
-180	- .56	- .55	- .56	- .38
-160	- .69	- .69	- .68	- .51
-140	- .81	- .81	- .80	- .63
-120	- .90	- .91	- .89	- .72
-100	- .98	-1.00	- .97	- .80
- 80	-1.05	-1.07	-1.04	- .86
- 60	-1.11	-1.13	-1.10	- .91
- 40	-1.15	-1.17	-1.15	- .95
- 20	-1.19	-1.21	-1.19	- .98
0	-1.22	-1.24	-1.22	-1.00
20	-1.24	-1.26	-1.24	-1.02
40	-1.25	-1.28	-1.26	-1.03
60	-1.27	-1.29	-1.27	-1.03
80	-1.28	-1.30	-1.28	-1.03
100	-1.29	-1.31	-1.29	-1.04
120	-1.30	-1.32	-1.29	-1.04
140	-1.32	-1.33	-1.30	-1.05
160	-1.34	-1.35	-1.31	-1.06
180	-1.36	-1.37	-1.32	-1.08
200	-1.39	-1.40	-1.33	-1.10

^aStandard deviation from a third degree polynomial fit is 0.02

^bStandard deviation from a third degree polynomial fit is 0.01

^cStandard deviation from a third degree polynomial fit is 0.03

^dStandard deviation from a third degree polynomial fit is 0.05

Table 9. dn/dT of CVD ZnS

Temperature (°C)	Wavelength (μm)		
	1.15 ^a	3.39 ^a	10.6 ^a
-180	3.5	2.8	2.7
-160	3.7	3.1	3.0
-140	3.8	3.3	3.3
-120	4.0	3.5	3.5
-100	4.1	3.7	3.7
- 80	4.2	3.9	3.8
- 60	4.3	4.0	3.9
- 40	4.4	4.1	4.0
- 20	4.5	4.1	4.0
0	4.5	4.2	4.1
20	4.6	4.2	4.1
40	4.6	4.3	4.1
60	4.7	4.3	4.1
80	4.7	4.3	4.1
100	4.7	4.3	4.2
120	4.8	4.4	4.2
140	4.8	4.4	4.3
160	4.9	4.4	4.4
180	4.9	4.5	4.5
200	5.0	4.6	4.7

^aStandard deviation from a third degree polynomial fit is 0.2

Table 10. dn/dT of CVD ZnSe ($10^{-5}K^{-1}$)

Temperature (°C)	Wavelength (μm)			
	0.6328 ^a	1.15 ^a	3.39 ^a	10.6 ^a
-180	7.6	5.4	5.0	4.9
-160	8.2	5.7	5.2	5.1
-140	8.7	6.0	5.4	5.4
-120	9.1	6.3	5.6	5.5
-100	9.4	6.5	5.8	5.7
-80	9.7	6.6	5.9	5.8
-60	10.0	6.7	6.0	5.9
-40	10.2	6.8	6.1	6.0
-20	10.3	6.9	6.1	6.0
0	10.5	7.0	6.2	6.1
20	10.6	7.0	6.2	6.1
40	10.7	7.0	6.2	6.1
60	10.8	7.1	6.3	6.1
80	10.9	7.1	6.3	6.2
100	11.0	7.2	6.3	6.2
120	11.1	7.2	6.4	6.3
140	11.3	7.3	6.4	6.3
160	11.5	7.4	6.5	6.4
180	11.8	7.6	6.6	6.6
200	12.1	7.8	6.7	6.7

^aStandard deviation from a third degree polynomial fit is 0.1

Table 11. Data Used in Computation of dn/dT

Material	Refractive Index, n_o				t_o (mm)	α
	632.8 nm	1.15 μ m	3.39 μ m	10.6 μ m		
BaF ₂	1.473 ^a	1.47 ^a	1.460 ^a	1.393 ^a	13.16	b
CaF ₂	1.433 ^c	1.43 ^c	1.416 ^c	-	13.41	b,d,e,f
KBr(RAP)	1.577 ^g	1.542 ^g	1.536 ^g	1.525 ^g	11.83	h
KCl(RAP)	1.488 ^j	1.478 ^j	1.473 ^j	1.454 ^j	11.87	h
LiF	1.392 ^k	1.386 ^k	1.360 ^k	-	5.59	h
NaF	1.325 ^l	1.321 ^l	1.312 ^l	-	12.21	h
SrF ₂	1.436 ^m	1.43 ⁿ	1.425 ⁿ	1.31 ⁿ	13.15	b
ZnS(CVD)	-	2.28 ^p	2.25 ^p	2.21 ^p	4.47	q,r
ZnSe(CVD)	2.590 ^s	2.47 ^s	2.436 ^s	2.403 ^s	17.49	q,r

^aI.H. Malitson, J. Opt. Soc. Amer. 54, 628 (1964).

^cI.H. Malitson, Appl. Opt. 2, 1103 (1963).

^eS.S. Sharma, Proc. Indian Acad. Sci. A31, 261 (1950).

^gR.E. Stephens, E.K. Plyler, W.S. Rodney & R.J. Spindler, J. Opt. Soc. Amer. 43, 111 (1953).

^jA. Feldman, D. Horowitz, R.M. Waxler, I.H. Malitson & M.J. Dodge, Optical Materials Characterization, NBSIR 76-1010 (Feb. 1976).

^lS.S. Ballard, J.S. Browder & J.F. Ebersole, in American Institute of Physics Handbook, Dwight E. Gray Ed. (McGraw-Hill Book Co., 1972) pp. 6-12 to 6-57.

ⁿEstimated

^qJ.S. Browder & S.S. Ballard, Appl. Optics 8, 793 (1969).

^bA.C. Bailey & B. Yates, Proc. Phys. Soc. 91, 390 (1967).

^dD.N. Batchelder & R.O. Simmons, J. Chem. Phys. 41, 2324 (1964).

^fS. Valentiner & J. Wallot, Ann. Phys., Lpz 46, 837 (1915).

^hR.K. Kirby, T.A. Hahn, & B.D. Rothrock, American Institute of Physics Handbook, Dwight E. Gray ed. (McGraw-Hill Book Co., 1972) pp 4-119 to 4-142.

^kL.W. Tilton & E.K. Plyler, J. Res. NBS 47, 25 (1951).

^mD.C. Stockbarger, OSRD Report No. 4690, Dec. 31, 1944.

^pReference [3].

^rData to be published in the next report.

^sA. Feldman, D. Horowitz, R.M. Waxler, I. Malitson & M.J. Dodge, Optical Materials Characterization, NBSIR 75-781 (Aug. 1975).

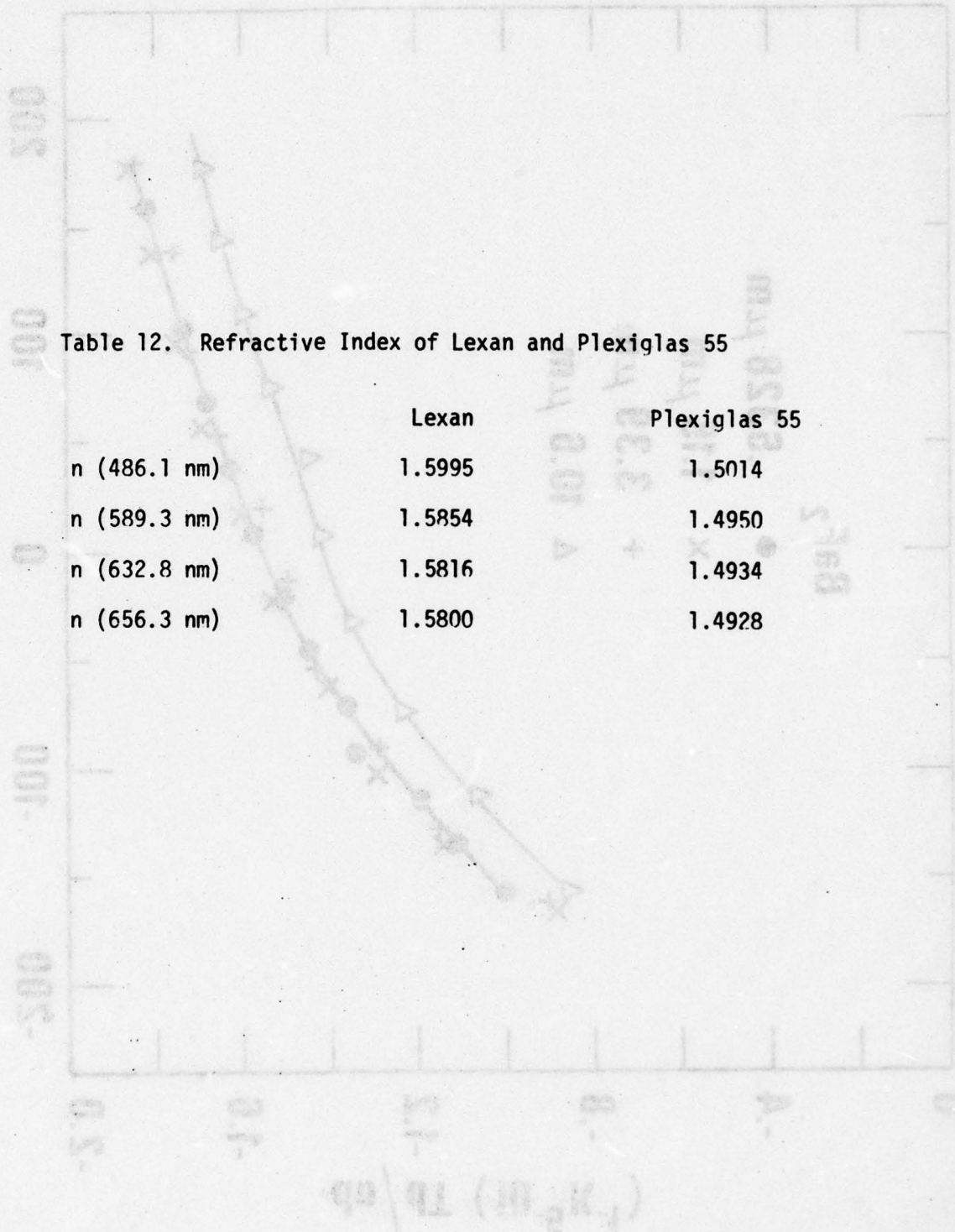


Table 12. Refractive Index of Lexan and Plexiglas 55

	Lexan	Plexiglas 55
n (486.1 nm)	1.5995	1.5014
n (589.3 nm)	1.5854	1.4950
n (632.8 nm)	1.5816	1.4934
n (656.3 nm)	1.5800	1.4928

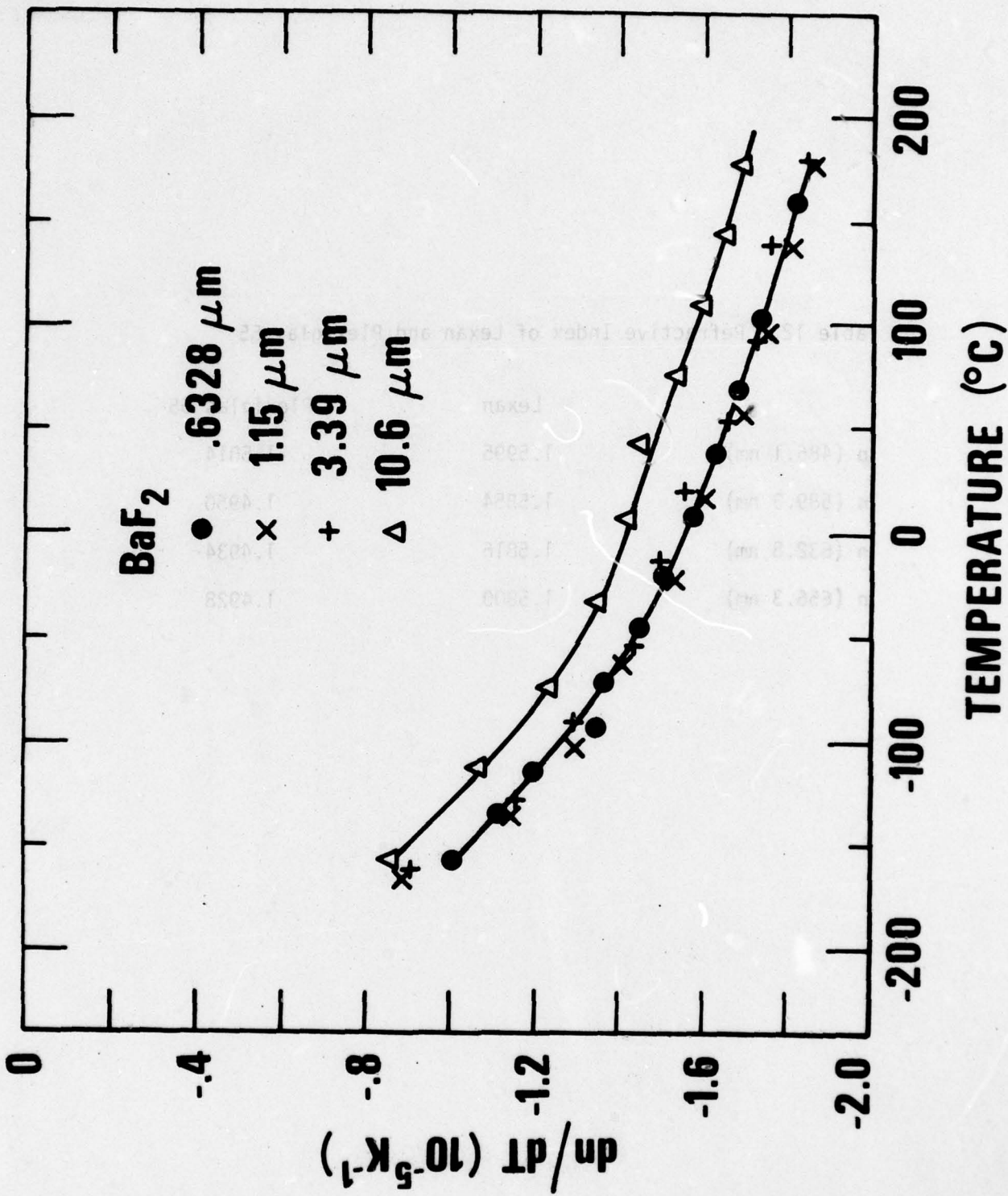


Fig. 4. $\frac{dn}{dT}$ of BaF₂ as a function of temperature.

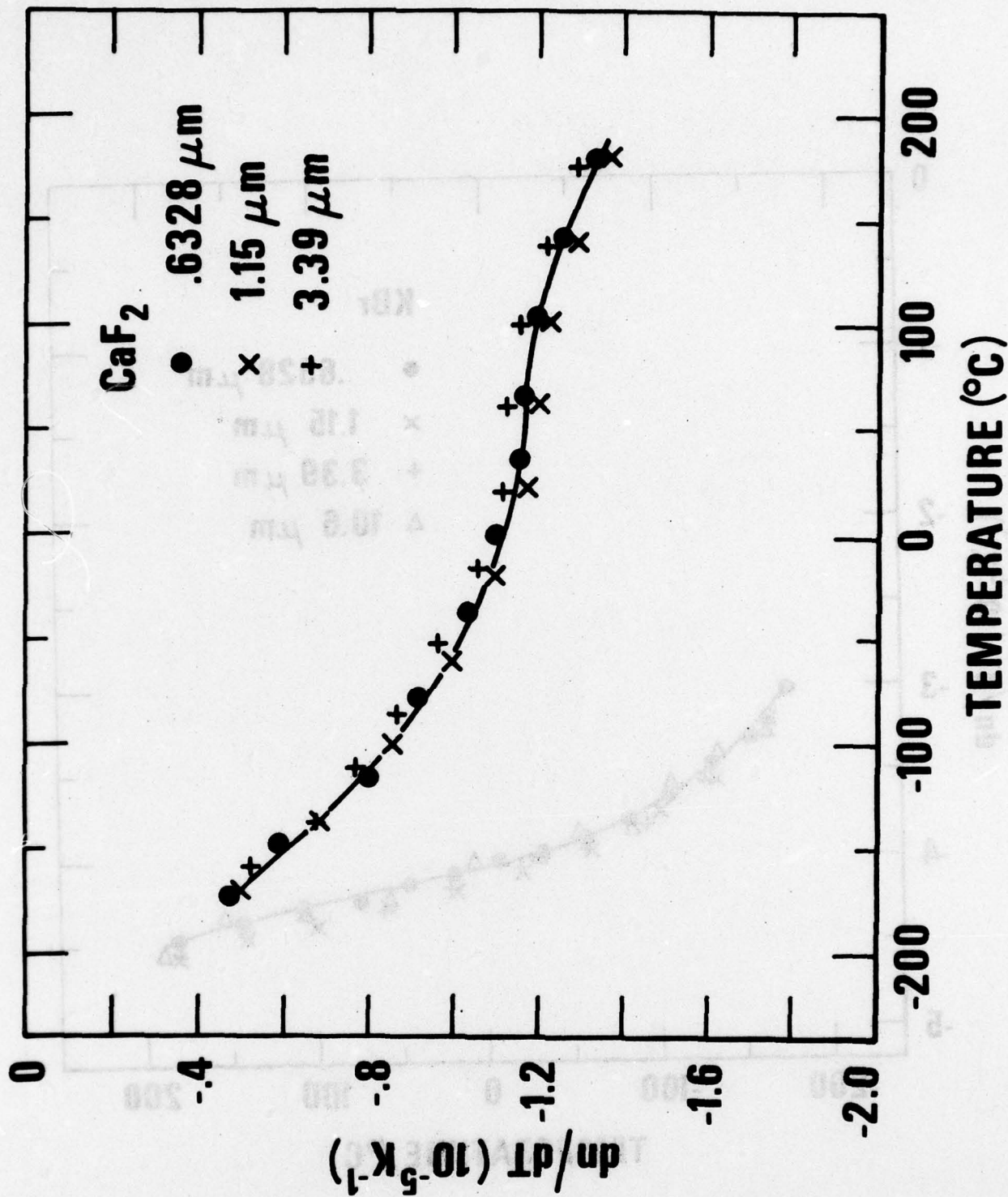


Fig. 5. dn/dT of CaF₂ as a function of temperature.

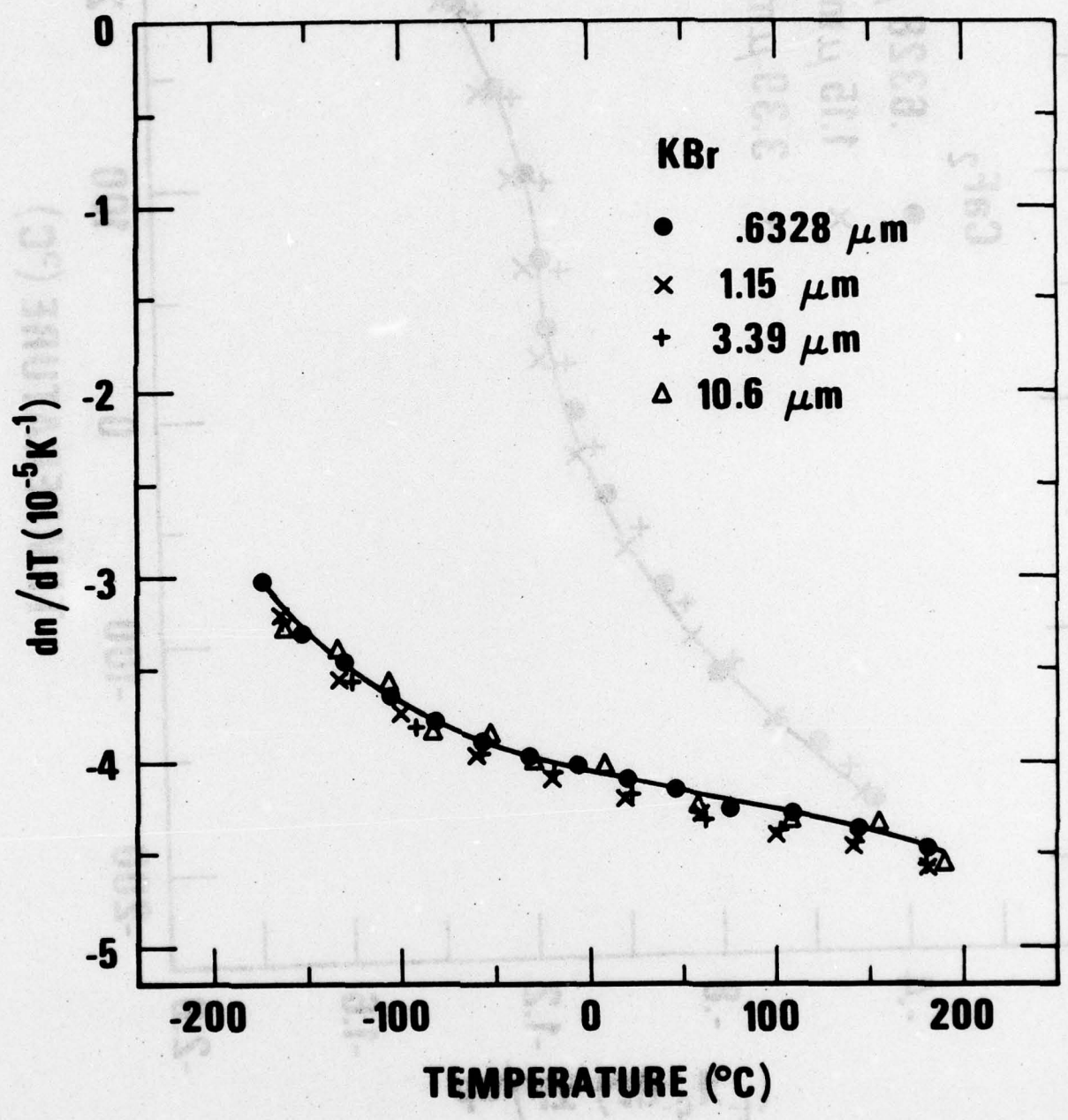


Fig. 6. dn/dT of KBr (RAP) as a function of temperature.

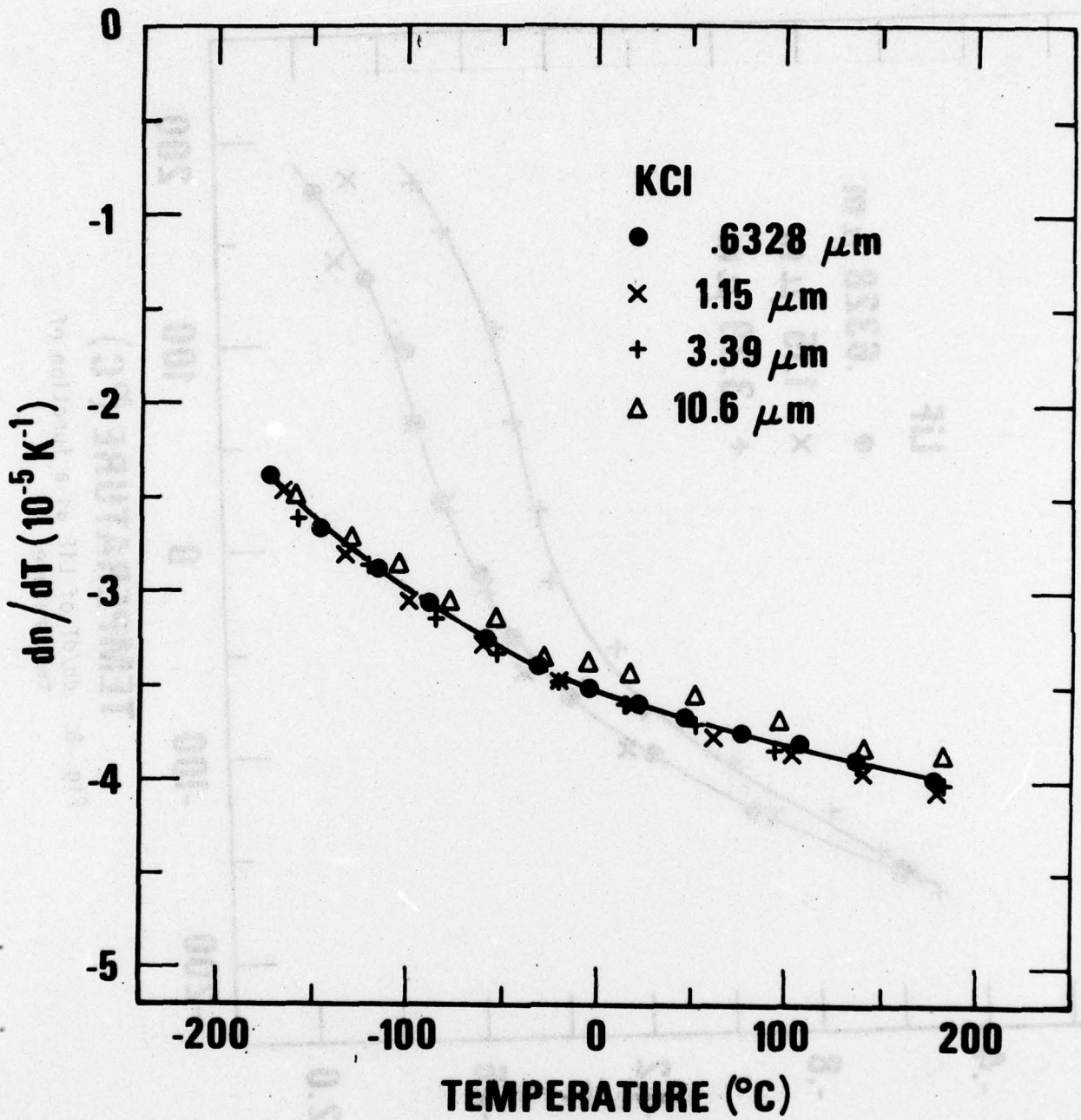


Fig. 7. dn/dT of KCl (RAP) as a function of temperature.

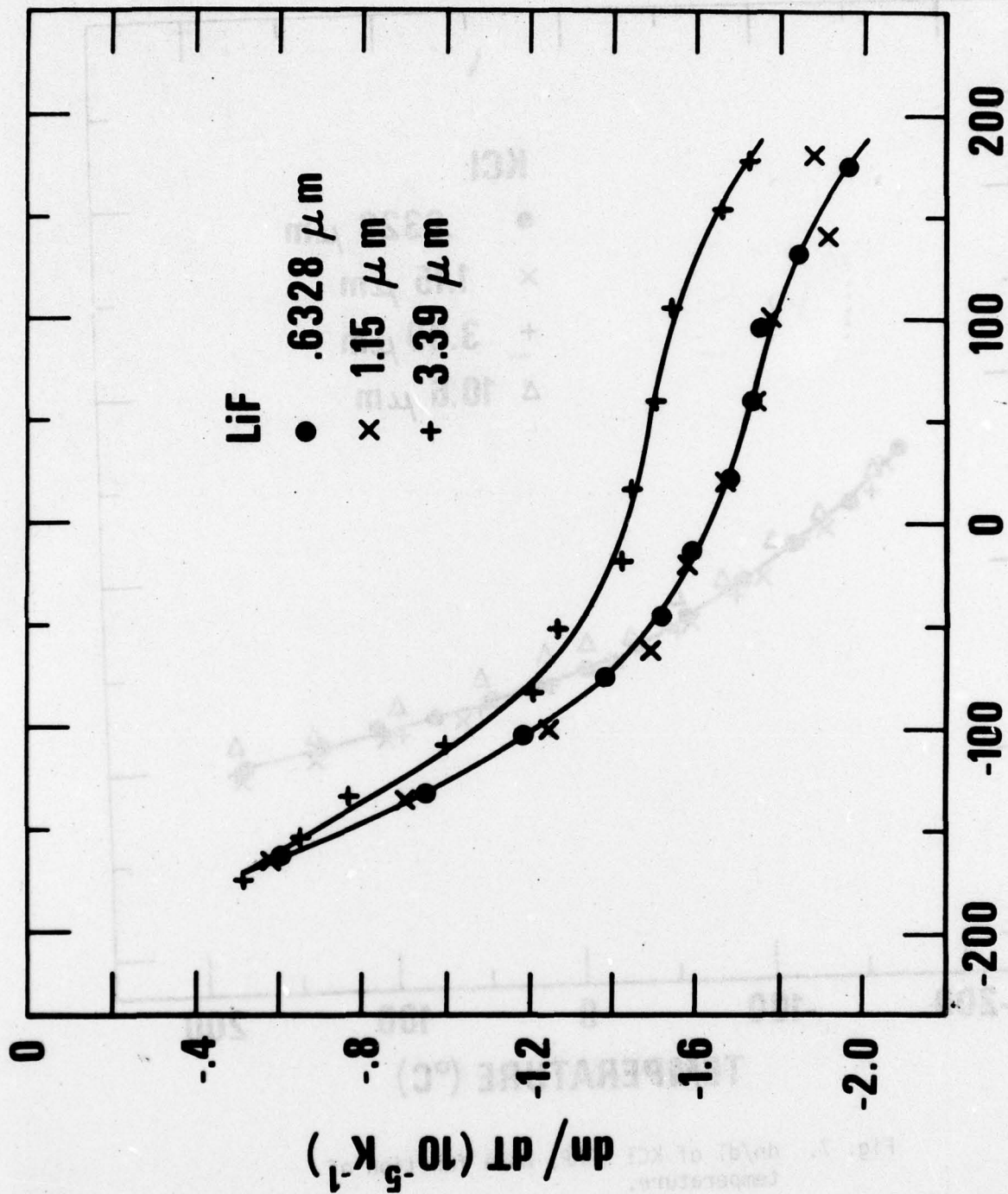


Fig. 8. dn/dT of LiF as a function of temperature.

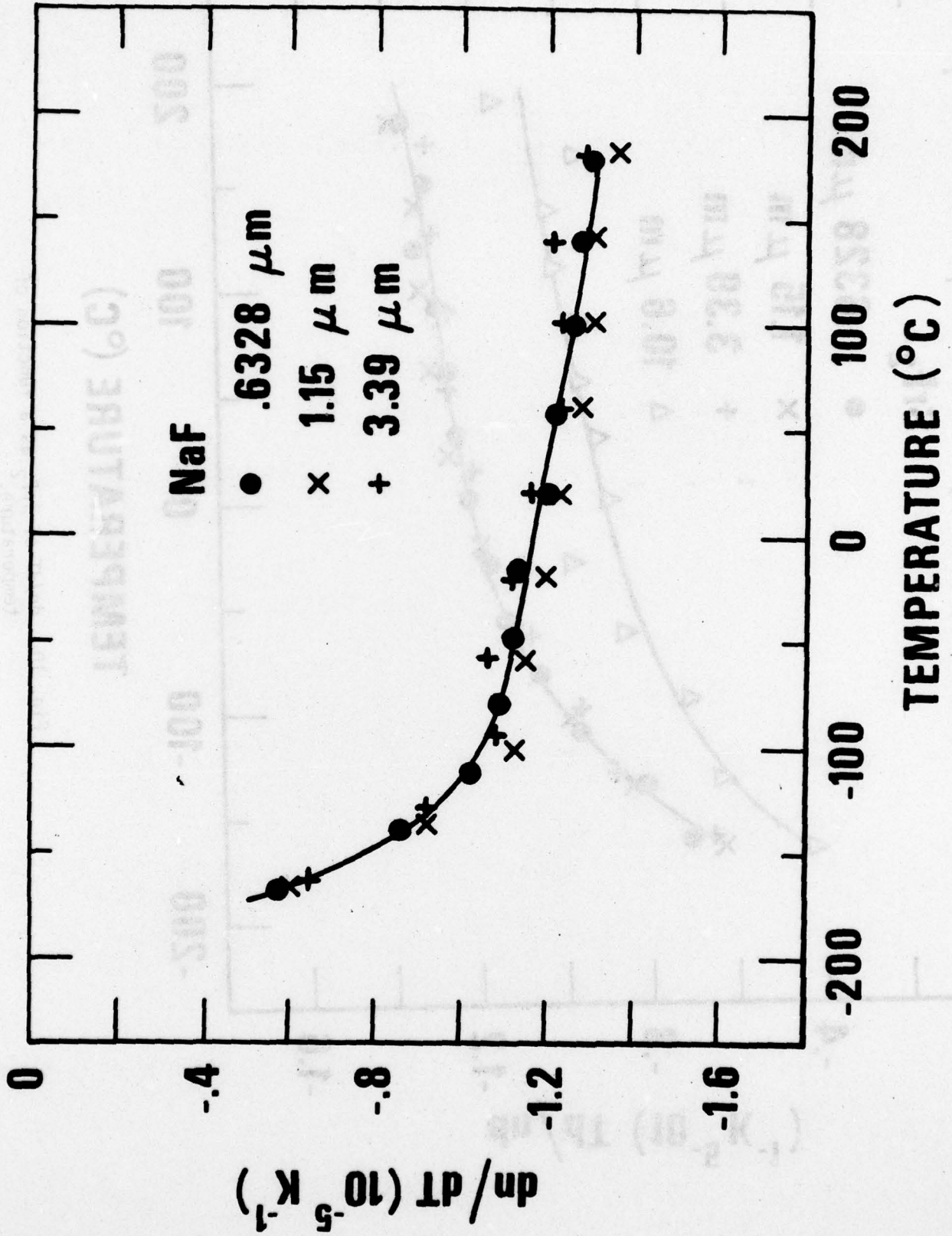


Fig. 9. dn/dT of NaF as a function of temperature.

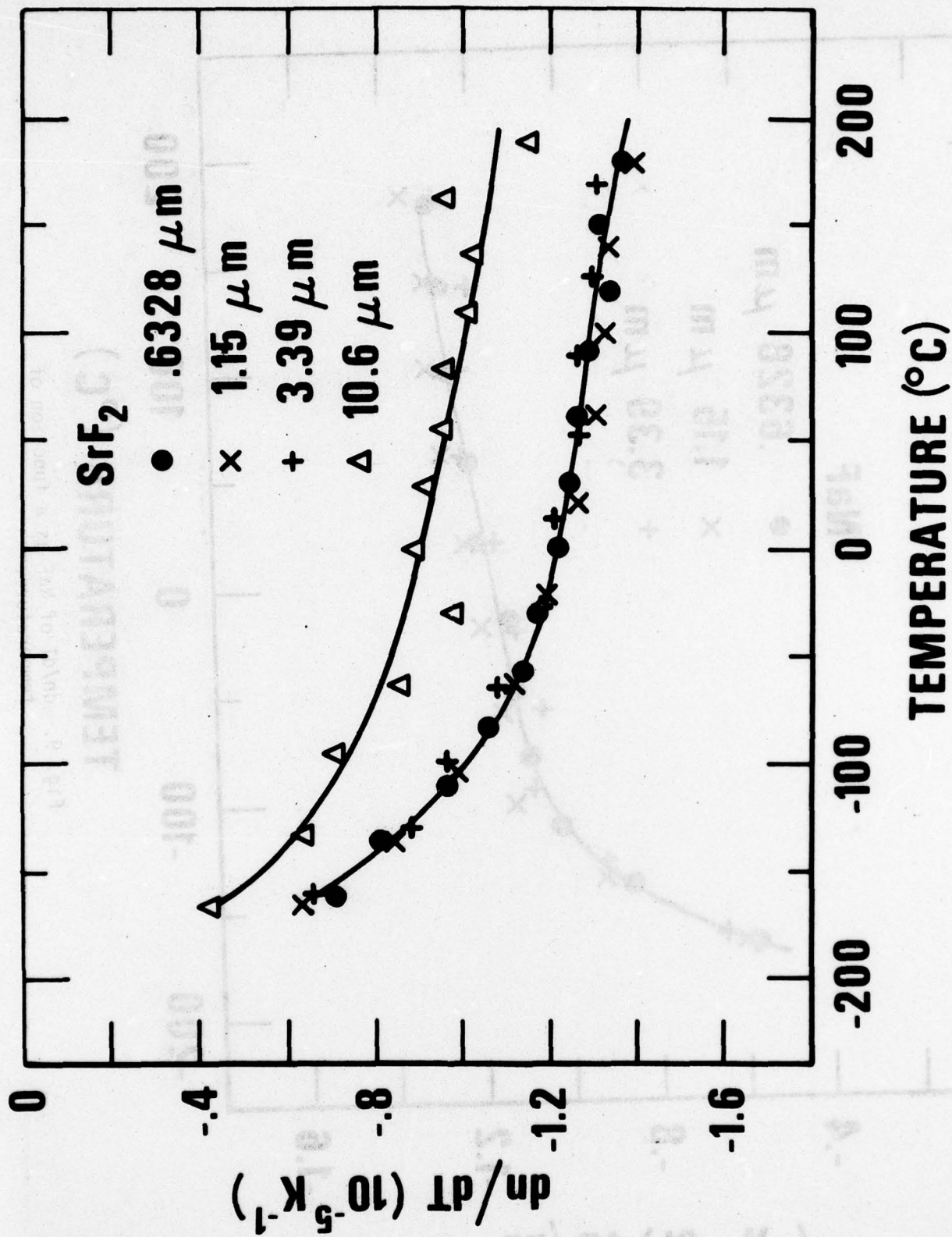


Fig. 10. dn/dT of SrF_2 as a function of temperature.

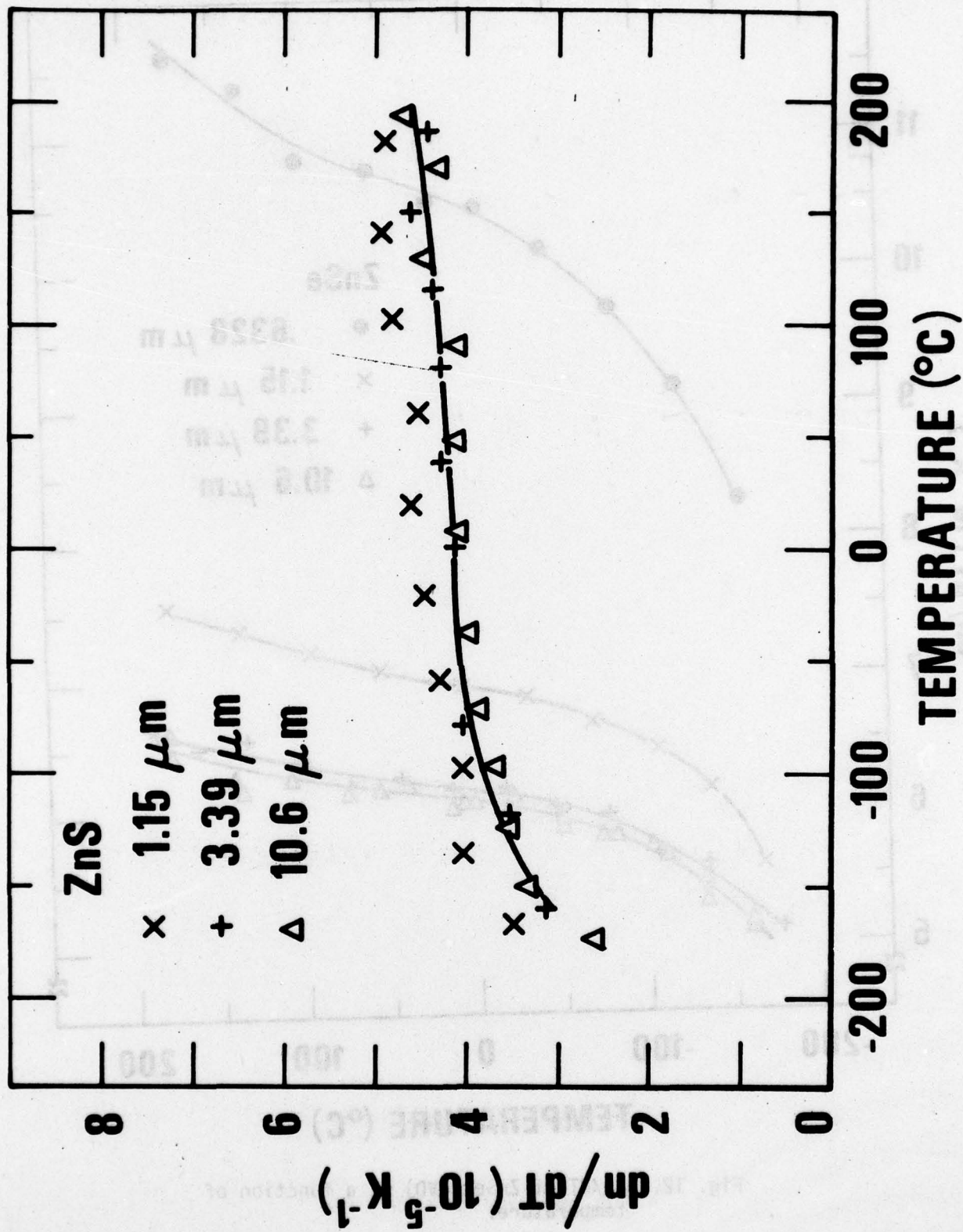


Fig. 11. dn/dT of ZnS (CVD) as a function of temperature.

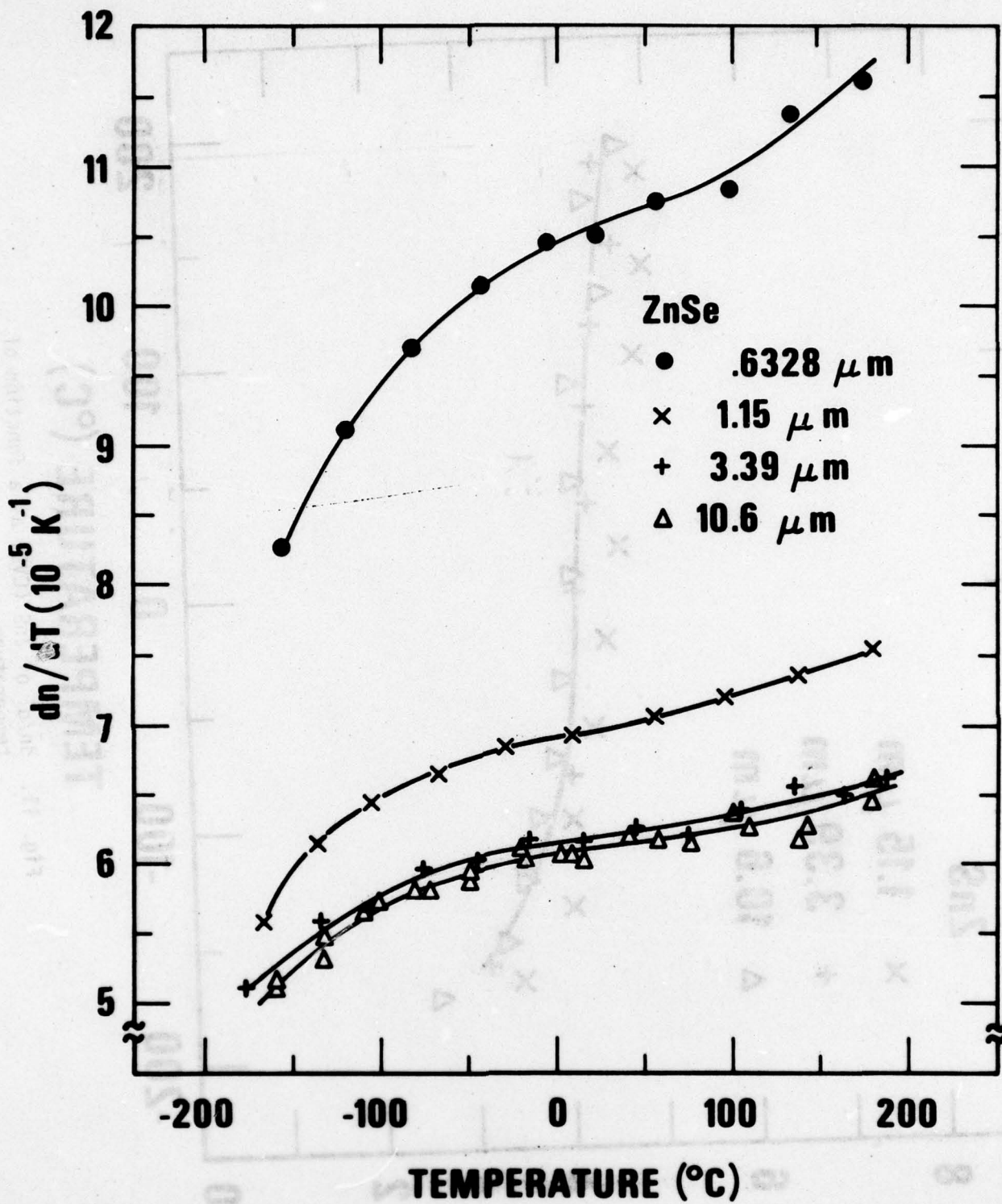


Fig. 12. dn/dT of ZnSe (CVD) as a function of temperature.

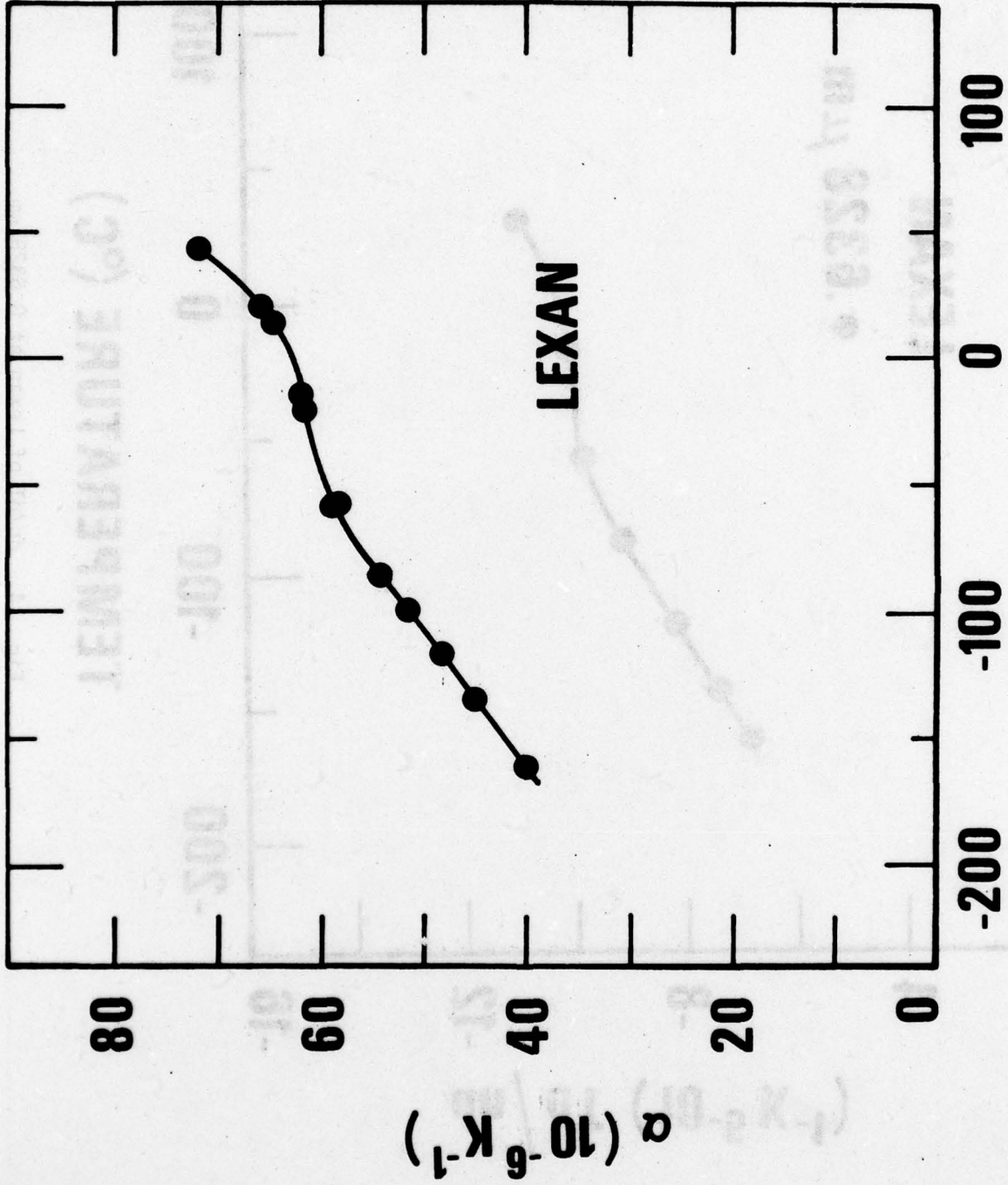


Fig. 13. Linear thermal expansion coefficient of Lexan as a function of temperature.

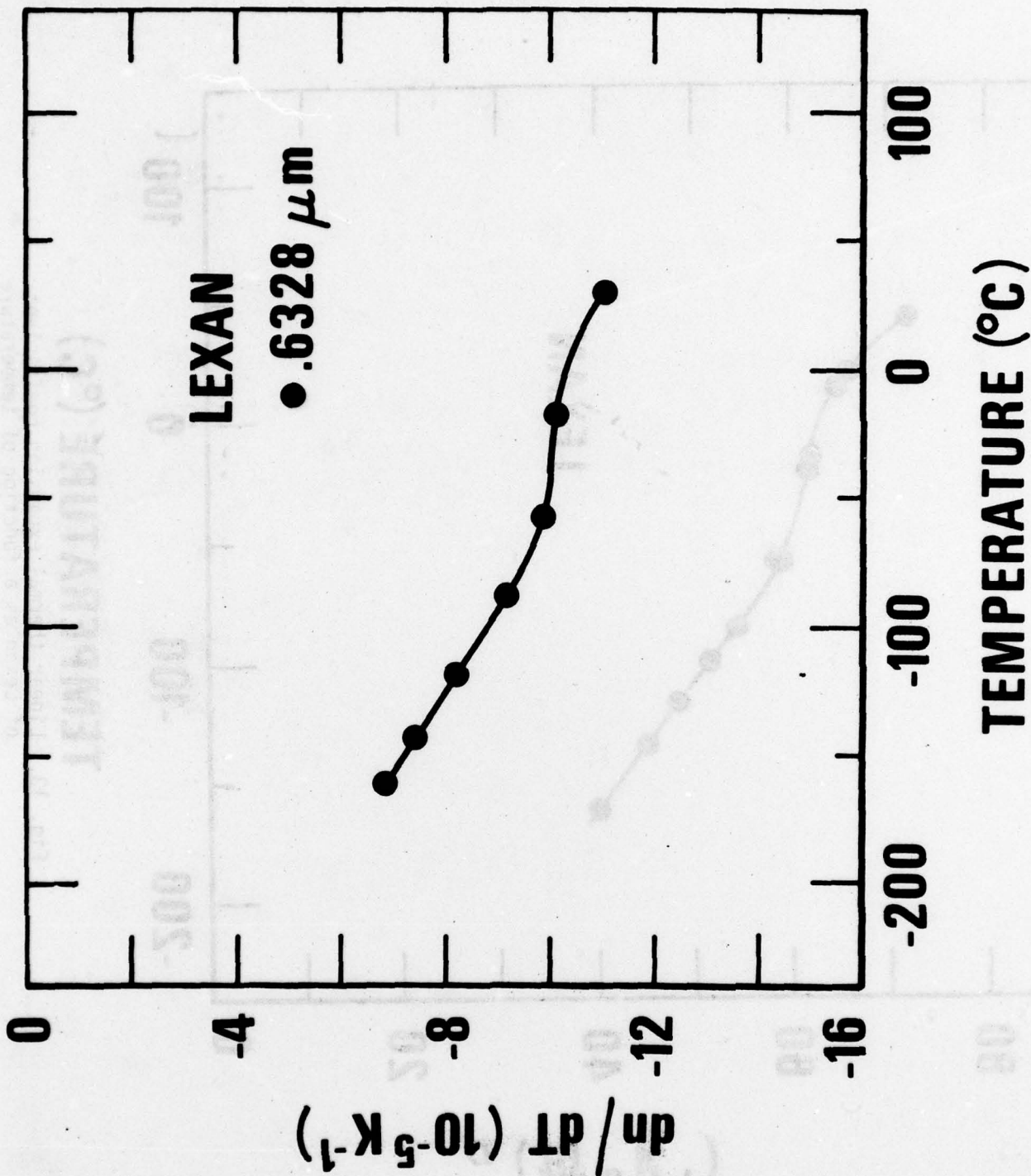


Fig. 14. dn/dT of Lexan at 0.6328 μm .

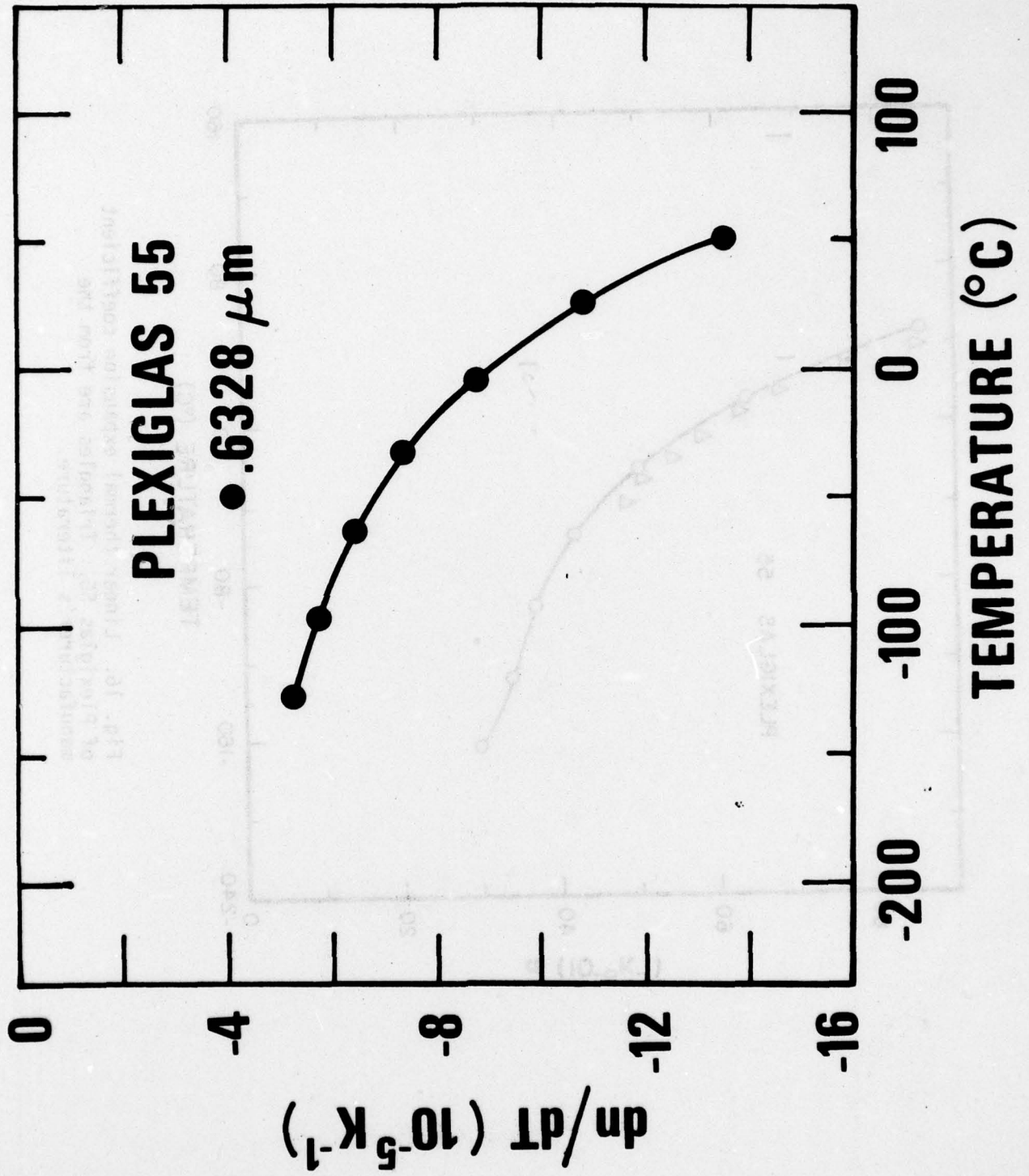


Fig. 15. dn/dT of Plexiglas 55 at 0.6328 μm .

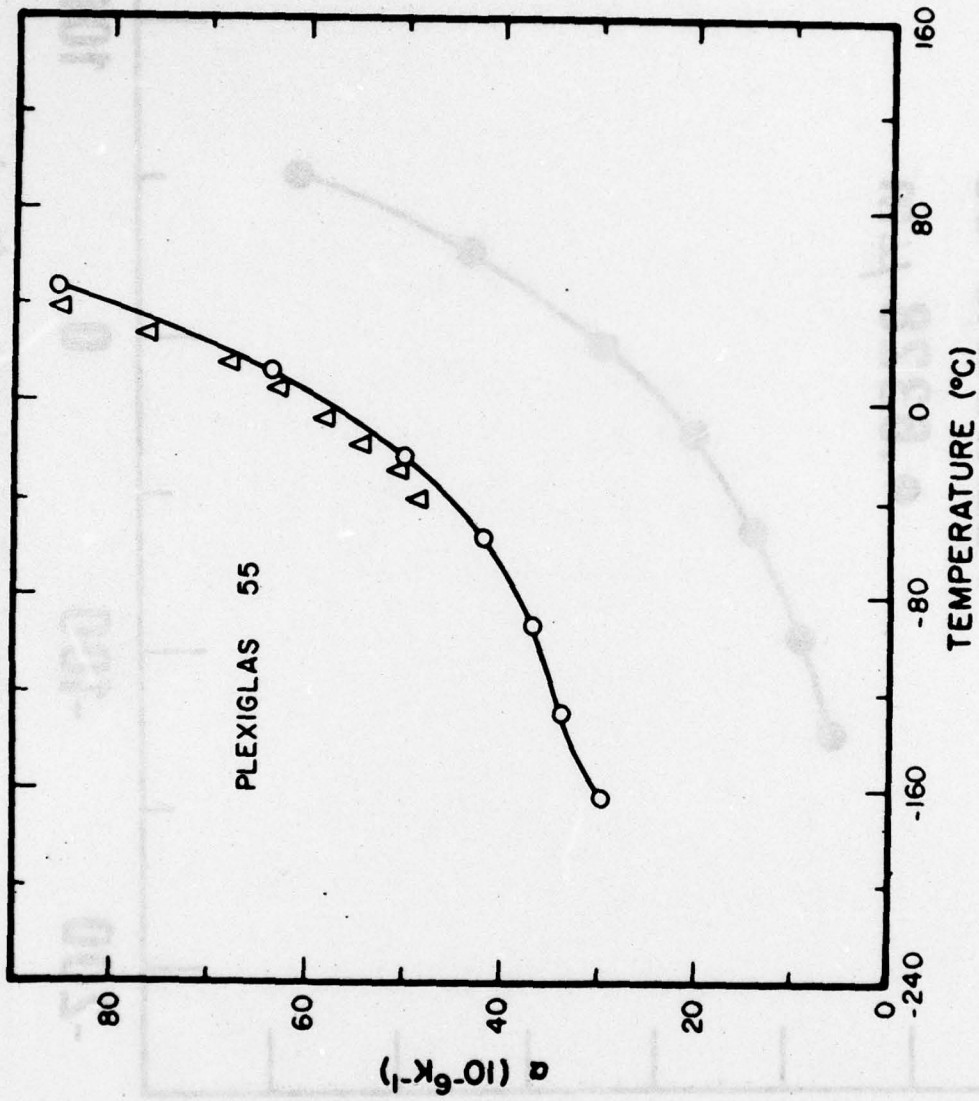


Fig. 16. Linear thermal expansion coefficient of Plexiglas 55. Triangles are from the manufacturer's literature.

3. Acknowledgments

We thank Dr. Phillip Klein of the Naval Research Laboratory for supplying the KCl (RAP) and KBr (RAP). The ZnS (CVD) was supplied by Raytheon. ZnSe (CVD) was provided both by Dr. Perry Miles of Raytheon and Dr. Carl Pitha of RADC. Polycrystalline CaF₂ was supplied by R. J. Harris of the University of Dayton Research Institute.

U.S. GOVERNMENT PRINTING OFFICE: 1964 O 352-134

1. TITLE AND SUBTITLE
2. AUTHOR(s)
3. PERFORMING ORGANIZATION NAME(S) AND ADDRESS(ES)
4. REPORT NUMBER
5. DISTRIBUTION STATEMENT (See Instructions for Authors)
6. PRICE (including postage and handling charges, where applicable)
7. AUTHORING AND PERFORMING ORGANIZATION REPORT NUMBER
8. PERFORMING ORGANIZATION REPORT NUMBER
9. PERFORMING ORGANIZATION REPORT NUMBER
10. PERFORMING ORGANIZATION REPORT NUMBER
11. PERFORMING ORGANIZATION REPORT NUMBER
12. PERFORMING ORGANIZATION REPORT NUMBER
13. PERFORMING ORGANIZATION REPORT NUMBER
14. PERFORMING ORGANIZATION REPORT NUMBER
15. PERFORMING ORGANIZATION REPORT NUMBER
16. PERFORMING ORGANIZATION REPORT NUMBER
17. PERFORMING ORGANIZATION REPORT NUMBER
18. PERFORMING ORGANIZATION REPORT NUMBER
19. PERFORMING ORGANIZATION REPORT NUMBER
20. PERFORMING ORGANIZATION REPORT NUMBER
21. PERFORMING ORGANIZATION REPORT NUMBER
22. PERFORMING ORGANIZATION REPORT NUMBER
23. PERFORMING ORGANIZATION REPORT NUMBER
24. PERFORMING ORGANIZATION REPORT NUMBER
25. PERFORMING ORGANIZATION REPORT NUMBER
26. PERFORMING ORGANIZATION REPORT NUMBER
27. PERFORMING ORGANIZATION REPORT NUMBER
28. PERFORMING ORGANIZATION REPORT NUMBER
29. PERFORMING ORGANIZATION REPORT NUMBER
30. PERFORMING ORGANIZATION REPORT NUMBER
31. PERFORMING ORGANIZATION REPORT NUMBER
32. PERFORMING ORGANIZATION REPORT NUMBER
33. PERFORMING ORGANIZATION REPORT NUMBER
34. PERFORMING ORGANIZATION REPORT NUMBER
35. PERFORMING ORGANIZATION REPORT NUMBER
36. PERFORMING ORGANIZATION REPORT NUMBER
37. PERFORMING ORGANIZATION REPORT NUMBER
38. PERFORMING ORGANIZATION REPORT NUMBER
39. PERFORMING ORGANIZATION REPORT NUMBER
40. PERFORMING ORGANIZATION REPORT NUMBER
41. PERFORMING ORGANIZATION REPORT NUMBER
42. PERFORMING ORGANIZATION REPORT NUMBER
43. PERFORMING ORGANIZATION REPORT NUMBER
44. PERFORMING ORGANIZATION REPORT NUMBER
45. PERFORMING ORGANIZATION REPORT NUMBER
46. PERFORMING ORGANIZATION REPORT NUMBER
47. PERFORMING ORGANIZATION REPORT NUMBER
48. PERFORMING ORGANIZATION REPORT NUMBER
49. PERFORMING ORGANIZATION REPORT NUMBER
50. PERFORMING ORGANIZATION REPORT NUMBER
51. PERFORMING ORGANIZATION REPORT NUMBER
52. PERFORMING ORGANIZATION REPORT NUMBER
53. PERFORMING ORGANIZATION REPORT NUMBER
54. PERFORMING ORGANIZATION REPORT NUMBER
55. PERFORMING ORGANIZATION REPORT NUMBER
56. PERFORMING ORGANIZATION REPORT NUMBER
57. PERFORMING ORGANIZATION REPORT NUMBER
58. PERFORMING ORGANIZATION REPORT NUMBER
59. PERFORMING ORGANIZATION REPORT NUMBER
60. PERFORMING ORGANIZATION REPORT NUMBER
61. PERFORMING ORGANIZATION REPORT NUMBER
62. PERFORMING ORGANIZATION REPORT NUMBER
63. PERFORMING ORGANIZATION REPORT NUMBER
64. PERFORMING ORGANIZATION REPORT NUMBER
65. PERFORMING ORGANIZATION REPORT NUMBER
66. PERFORMING ORGANIZATION REPORT NUMBER
67. PERFORMING ORGANIZATION REPORT NUMBER
68. PERFORMING ORGANIZATION REPORT NUMBER
69. PERFORMING ORGANIZATION REPORT NUMBER
70. PERFORMING ORGANIZATION REPORT NUMBER
71. PERFORMING ORGANIZATION REPORT NUMBER
72. PERFORMING ORGANIZATION REPORT NUMBER
73. PERFORMING ORGANIZATION REPORT NUMBER
74. PERFORMING ORGANIZATION REPORT NUMBER
75. PERFORMING ORGANIZATION REPORT NUMBER
76. PERFORMING ORGANIZATION REPORT NUMBER
77. PERFORMING ORGANIZATION REPORT NUMBER
78. PERFORMING ORGANIZATION REPORT NUMBER
79. PERFORMING ORGANIZATION REPORT NUMBER
80. PERFORMING ORGANIZATION REPORT NUMBER
81. PERFORMING ORGANIZATION REPORT NUMBER
82. PERFORMING ORGANIZATION REPORT NUMBER
83. PERFORMING ORGANIZATION REPORT NUMBER
84. PERFORMING ORGANIZATION REPORT NUMBER
85. PERFORMING ORGANIZATION REPORT NUMBER
86. PERFORMING ORGANIZATION REPORT NUMBER
87. PERFORMING ORGANIZATION REPORT NUMBER
88. PERFORMING ORGANIZATION REPORT NUMBER
89. PERFORMING ORGANIZATION REPORT NUMBER
90. PERFORMING ORGANIZATION REPORT NUMBER
91. PERFORMING ORGANIZATION REPORT NUMBER
92. PERFORMING ORGANIZATION REPORT NUMBER
93. PERFORMING ORGANIZATION REPORT NUMBER
94. PERFORMING ORGANIZATION REPORT NUMBER
95. PERFORMING ORGANIZATION REPORT NUMBER
96. PERFORMING ORGANIZATION REPORT NUMBER
97. PERFORMING ORGANIZATION REPORT NUMBER
98. PERFORMING ORGANIZATION REPORT NUMBER
99. PERFORMING ORGANIZATION REPORT NUMBER
100. PERFORMING ORGANIZATION REPORT NUMBER

⑨ Semi-annual technical rept.
1 Feb - 31 Jul 77

14

1. U.S. DEPT. OF COMM. BIBLIOGRAPHIC DATA SHEET		2. Gov't Accession No.		3. Recipient's Accession No.	
4. TITLE AND SUBTITLE		5. Publication Date		6. Performing Organization Code	
② OPTICAL MATERIALS CHARACTERIZATION.					
7. AUTHOR(S)		8. Performing Organ. Report No.		10. Project/Task/Work Unit No.	
⑩ Albert/Feldman, Deane/Horowitz, Roy M./Maxler, Marilyn J./Dodge and Warren K./Gladden				3130442	
9. PERFORMING ORGANIZATION NAME AND ADDRESS		11. Contract/Grant No.			
NATIONAL BUREAU OF STANDARDS DEPARTMENT OF COMMERCE WASHINGTON, D.C. 20234		⑪ Aug 77			
12. Sponsoring Organization Name and Complete Address (Street, City, State, ZIP)		13. Type of Report & Period Covered		14. Sponsoring Agency Code	
Advanced Research Projects Agency Arlington, Virginia 22209					
15. SUPPLEMENTARY NOTES					
⑮ WARPA Order - 2620					
16. ABSTRACT (A 200-word or less factual summary of most significant information. If document includes a significant bibliography or literature survey, mention it here.)					
<p>The refractive index of fusion cast CaF₂ was measured at room temperature over the wavelength range 0.2144 μm to 8.662 μm and the data were fitted to a Selmeier type equation. Measurements of refractive index of hot forged CaF₂ were extended to the wavelength range 0.2024 μm to 0.2483 μm. Data are presented for dn/dT of single crystal specimens of CaF₂, BaF₂, reactive atmosphere processed (RAP) KCl and KBr, LiF, NaF, and SrF₂, and polycrystalline chemical vapor deposited (CVD) ZnSe and ZnS. The measurements were done by the method of Fizeau interferometry over the temperature range -180° to 200 °C at the wavelengths 0.6328 μm, 1.15 μm, 3.39 μm and 10.6 μm. Data are presented for the refractive indices, the linear thermal expansion and dn/dT of Lexan and Plexiglas 55.</p> <p style="text-align: center;">* micrometers</p>					
17. KEY WORDS (six to twelve entries; alphabetical order; capitalize only the first letter of the first key word unless a proper name; separated by semicolons) BaF ₂ ; CaF ₂ ; KBr; KCl; Lexan; LiF; NaF; Plexiglas 55; refractive index; SrF ₂ ; thermal coefficient of refractive index; ZnS; ZnSe.					
18. AVAILABILITY		19. SECURITY CLASS (THIS REPORT)		21. NO. OF PAGES	
<input type="checkbox"/> For Official Distribution. Do Not Release to NTIS <input type="checkbox"/> Order From Sup. of Doc., U.S. Government Printing Office Washington, D.C. 20402, SD Cat. No. C13 <input checked="" type="checkbox"/> Order From National Technical Information Service (NTIS) Springfield, Virginia 22151		UNCLASSIFIED		42	
		20. SECURITY CLASS (THIS PAGE)		22. Price	
		UNCLASSIFIED		\$4.00	

16 240 800 -